Live Approach Exposure for EOD Responders: Overpressure, Impulse, and Fragment-Hit Probability in Real Time

Bomb Doctor

The Long Walk Technical Series, Paper 2

June 21, 2026

Abstract

A cordon describes the hazard around a device. It does not tell a responder how their own exposure changes as they close on the incident. This paper develops the live approach-exposure model behind The Long Walk display. Given the responder's position and the incident parameters, the model reports distance, bearing, the overpressure the responder is standing in, the probability of being struck by a hazardous fragment, the positive-phase impulse, and a blast-lung lethality estimate that accounts for impulse rather than peak pressure alone. We give the closed-form models with their assumptions and validity bands, derive the fragment-hit probability from areal density, and present the injury correlations as probit functions anchored to the published blast-injury literature. Seven figures, each generated from the shipped code, characterise the model: the overpressure profile against injury bands, eardrum rupture probability, fragment-hit probability, positive-phase impulse, the divergence between pressure-only and impulse-aware lethality, the combined banded exposure level, and the position-smoothing response. The model runs on a wrist-worn device updating on a live position fix, and we describe the smoothing that keeps the readout stable where the overpressure curve is steepest, together with the lag it costs. A central finding is that pressure-only lethality models over-state the risk for smaller charges, because they ignore the short positive-phase pulse. As with the rest of the series, the model is a documented engineering tool and not operational guidance.

Model status and limitations

The quantitative models in this paper are open-literature engineering correlations implemented in software. Fragment-distance and injury correlations are *illustrative* estimates for cordon sizing, not guarantees; real outcomes depend on casing, terrain, geometry, and orientation not known in the field. All distances default to the greater of the computed value and the published doctrinal floor. Nothing here is operational guidance or a substitute for command explosive-safety authority.

1 Introduction

The companion paper in this series sizes a cordon around an incident (U.S. Department of Defense, 2019), and validates that cordon model against the conventional tools an EOD team already carries, the bare K-factor calculator and the DHS/ATF standoff card (U.S. Department of Homeland Security & Bureau of Alcohol, Tobacco, Firearms and Explosives, 2016), reproducing them where overpressure governs and extending them where fragmentation does. This paper addresses a different question, the one a responder actually asks while moving toward a device: what is happening to me, here, right now, as I approach. Distance and bearing answer where the incident is. They do not answer how much overpressure the responder is exposed to at the

present range, how likely a hazardous-fragment strike is at that range, or how those quantities are changing with each step inward. The approach-exposure model answers those questions continuously, from a live position fix, and surfaces them on a wrist-worn display.

The motivation is that exposure is not monotone in the quantities a responder can see directly. A responder can read distance off a map, but distance alone hides two effects that dominate close in. The first is that air-blast overpressure rises steeply, faster than the inverse of distance, as the charge is approached, so the last few tens of metres carry most of the blast risk. The second is that fragment-hit probability rises even faster, as the inverse square of range inside the hazard band, so a responder can be in serious fragment danger while standing in mild overpressure. Neither effect is visible from a distance readout. Both are central to a safe approach.

The design is shaped by the device. The model runs on a wrist-worn display with a noisy satellite position fix and limited computation. Two consequences follow. First, because the overpressure curve is nearly vertical close to the charge, raw position jitter of a few metres would swing the displayed overpressure by hundreds of kilopascals. The readout must be stabilised without distorting the underlying physics. Second, every quantity must be cheap to evaluate at the display refresh rate, and each must degrade gracefully outside the validity band of its correlation rather than returning a misleading extrapolation. We address both directly.

The contribution of this paper is not a new physical theory. It is the assembly, derivation, and software-traceable implementation of established blast-injury and fragment-hazard correlations into a single live exposure picture, the demonstration of two effects that change responder behaviour, the steep inverse-square rise of fragment risk inside a cordon and the over-statement of pressure-only lethality for small charges, and the description of the smoothing that makes the picture usable on the wrist. The remainder of the paper is organised as follows. Section 2 reviews the blast-injury and fragment-hazard literature. Section 3 derives the model. Section 4 presents results and validation from the shipped code. Section 5 describes the implementation and its traceability. Section 6 states the limitations, and Sections 7 and 8 close.

2 Background and Related Work

2.1 Blast-injury biomechanics

The human response to air blast has been studied since the mid twentieth century, and the resulting thresholds and iso-risk curves are the foundation of the model here. Primary blast injury, the injury caused by the pressure wave itself rather than by fragments or displacement, concentrates in the gas-containing organs, the ear and the lung (Baker et al., 1983; Glasstone & Dolan, 1977). The tympanic membrane is the most sensitive structure, with rupture beginning at overpressures far below those that threaten the lung, which makes eardrum response a useful early indicator of exposure even where life-threatening injury is absent.

Lung injury is the dominant lethal mechanism of primary blast. The classic work of Bowen et al. (1968) established survival and lethality curves for the lung as functions of both peak overpressure and positive-phase duration, recognising that a short, intense pulse and a longer, milder one are not equivalent. This duration dependence, equivalently an impulse dependence, is the single most important refinement over a peak-pressure-only description, and it is the reason a small charge and a large charge that produce the same peak pressure at a point can carry very different lung-lethality.

2.2 Peak pressure versus impulse

A peak-pressure-only injury model treats the wave as fully described by its maximum. For large charges, where the positive phase is long, this is a reasonable approximation. For small charges it is not, because the positive phase is short and the lung integrates pressure over time. The

Bowen iso-risk surface (Bowen et al., 1968) encodes this through a combination of an effective pressure, which accounts for the orientation and reflection of the subject, and a scaled impulse, normalised by ambient pressure and body mass. A survey of probit functions for blast injury compiled by the European Commission Joint Research Centre (Karlos et al., 2019) expresses these curves in a form convenient for implementation, and we follow that formulation. The practical consequence, developed in Section 4, is that the impulse-aware estimate is markedly lower than the pressure-only estimate across a wide near-field band, and that the gap widens as the charge gets smaller.

2.3 Fragment hazard

Cased charges produce fragments that travel well beyond the air-blast hazard. Explosive-safety practice characterises fragment hazard through areal density, the number of hazardous fragments per unit area at a given range, and defines the hazardous fragment distance (HFD) as the range at which that density falls to one hazardous fragment per $600\,\mathrm{ft}^2$, the accepted personnel criterion (Department of Defense Explosives Safety Board, 2009). A hazardous fragment is conventionally one carrying at least 58 ft-pounds of kinetic energy, the threshold associated with a serious wounding capability. Because areal density falls roughly as the inverse square of range, the probability that a responder is struck rises sharply as the HFD is approached from outside, which is the behaviour the model must surface.

2.4 Probit methodology

Injury probabilities in this work are expressed as probit functions, the standard dose-response form in which a probability is obtained by passing a log-dose through a normal cumulative distribution (Baker et al., 1983; Karlos et al., 2019). Probit functions are convenient because they are monotone, bounded, and parameterised by a median and a slope, and because the blast-injury literature reports its iso-risk curves in this form. We use probit forms for eardrum rupture and for pressure-only lethality, and the Bowen impulse-aware form for the lung.

3 Model

3.1 Geometry

Let the responder be at latitude and longitude (ϕ_1, λ_1) and the incident at (ϕ_2, λ_2). The model computes the great-circle distance with the haversine formula and the initial true bearing with the standard forward-azimuth formula on a spherical Earth of radius $R_\oplus = 6371\,\mathrm{km}$. These are standard and are stated here only for completeness:

$$a = \sin^2\frac{\Delta\phi}{2} + \cos\phi_1 \cos\phi_2 \sin^2\frac{\Delta\lambda}{2}, \qquad d = 2R_\oplus \,\mathrm{atan2}\Big(\sqrt{a}, \sqrt{1-a}\Big), \tag{1}$$

$$\theta = \mathrm{atan2}\big(\sin\Delta\lambda\cos\phi_2,\ \cos\phi_1\sin\phi_2 - \sin\phi_1\cos\phi_2\cos\Delta\lambda\big). \tag{2}$$

The spherical approximation is adequate at the scales of an EOD approach, where the responder and the incident are at most a few kilometres apart and the error from neglecting the ellipsoid is far below the position-fix error.

3.2 Overpressure and injury-band classification

The model evaluates peak incident overpressure p_s at the responder's range from the same air-blast correlation used for cordon sizing in Paper 1, with a near-field clamp at the correlation's validity floor so the curve never diverges (Brode, 1955; Mills, 1987). The overpressure is then

classified into a named injury band at the thresholds in Table 1, drawn from the blast-injury literature (Baker et al., 1983; Glasstone & Dolan, 1977). The bands give the responder a qualitative reading that does not depend on a precise charge estimate. Figure 1 shows the overpressure profile for a representative 1000 kg charge with the bands shaded.

Table 1. Overpressure injury-band thresholds used by the exposure model. Values are nominal onsets from the blast-injury literature and are rounded for display.

Band	Onset (kPa)	Approximate effect
Structural / glass	6.9	Window breakage; public standoff basis
Eardrum rupture onset	34.5	Onset of tympanic rupture
Eardrum rupture 50 %	103	Half of exposed eardrums rupture
Serious lung injury	83	Onset of significant pulmonary injury
Potentially lethal	200	Lower bound of the lethal band
Lethal 50 %	280	Half of exposed personnel
Lethal 99 %	350	Near-certain lethality

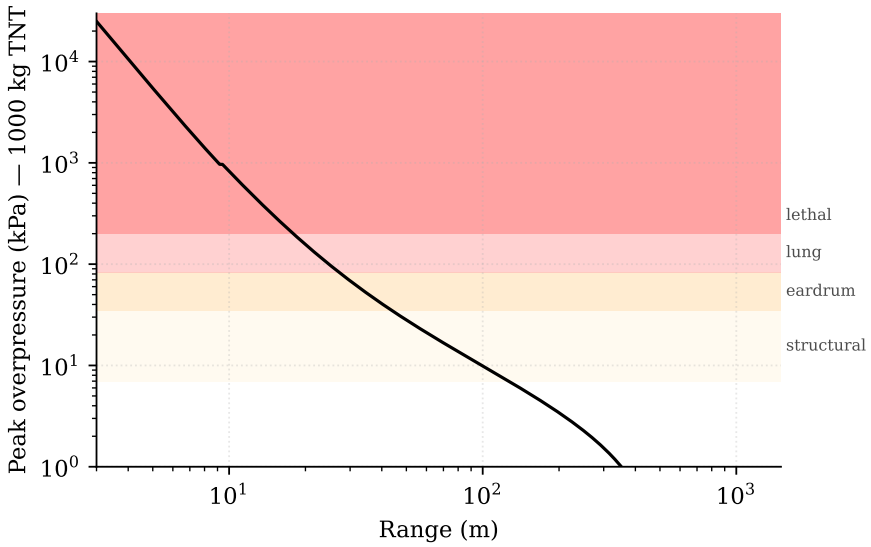

Figure 1. Overpressure versus range for 1000 kg TNT with injury bands shaded, generated from the shipped model. The steep near-field rise is the reason a distance readout alone understates how fast exposure grows on approach.

3.3 Eardrum rupture probability

Eardrum rupture probability is modelled as a log-normal probit anchored at the onset and the fifty-percent thresholds of Table 1. Writing Φ for the standard normal cumulative distribution, the probability at overpressure p is

$$P_{\mathrm{ear}}(p) = \Phi\!\left(\frac{\ln p - \ln p_{50}}{\sigma}\right), \qquad \sigma = \frac{\ln(p_{50}/p_{\mathrm{onset}})}{1.645}, \tag{3}$$

with $p_{50} = 103\,\mathrm{kPa}$ and $p_{\mathrm{onset}} = 34.5\,\mathrm{kPa}$, so that the onset corresponds to roughly the five-percent point. Eardrum response is reported continuously because it provides a graded indicator across the band where lung injury is still absent. Figure 2 shows the curve for three charge sizes.

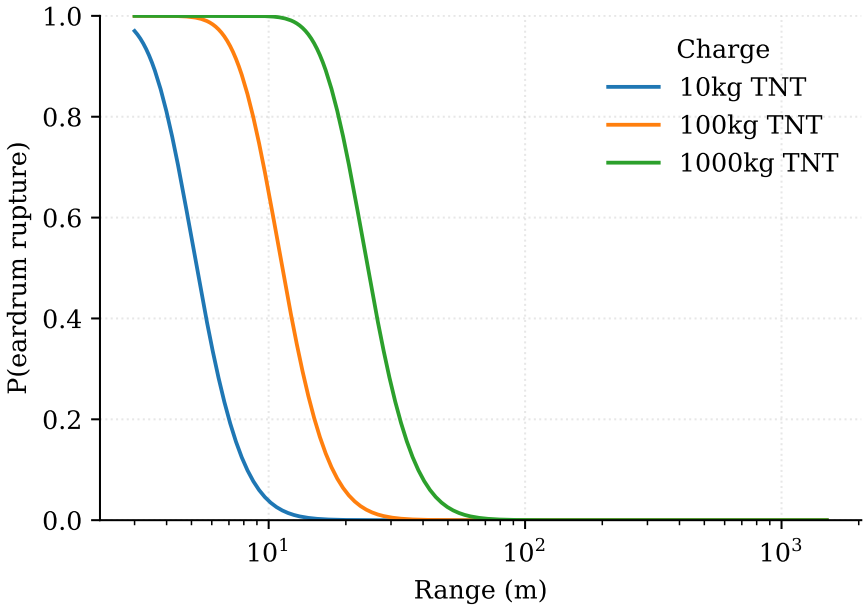

Figure 2. Eardrum rupture probability versus range for three charge sizes, from the probit of Equation 3 as implemented.

3.4 Fragment-hit probability

Inside the fragment hazard range, the model reports the probability that the responder is struck by a hazardous fragment. We model hazardous fragments as a spatial Poisson process whose areal density $\rho(R)$ falls as the inverse square of range, anchored so that at the HFD the density gives the defined criterion of one hazardous fragment per 600 ft^2, which corresponds to a hit probability of approximately one percent for a standing person (Department of Defense Explosives Safety Board, 2009). For a Poisson field, the probability of at least one hit over the presented area is $1 - \exp(-\rho A)$. Folding the inverse-square density and the anchor into a single constant gives the compact form the device evaluates,

$$P_{\mathrm{hit}}(R) = 1 - \exp\left[-0.0104 \left(\frac{\mathrm{HFD}}{R}\right)^2\right]. \tag{4}$$

The constant 0.0104 sets $P_{\mathrm{hit}}(\mathrm{HFD}) \approx 0.01$, consistent with the density criterion. Figure 3 shows the probability for several HFD anchors. The inverse-square argument means fragment risk rises steeply in the last tens of metres, well inside any blast cordon, which is the behaviour a responder most needs surfaced.

3.5 Positive-phase impulse

Peak overpressure alone is an incomplete predictor of blast-lung injury, because the lung integrates the pressure history over the positive phase. The model evaluates the positive-phase incident specific impulse from the Kingery-Bulmash parametrisation (Kingery & Bulmash, 1984), which expresses scaled impulse as a piecewise polynomial in the logarithm of the scaled distance $Z = R/W^{1/3}$, valid over a defined band of Z. Outside that band the parametrisation returns no value and the model suppresses the impulse-dependent output rather than extrapolating. Figure 4 shows the impulse field for three charge sizes. The cube-root scaling is again visible as a near-constant vertical offset between curves on logarithmic axes.

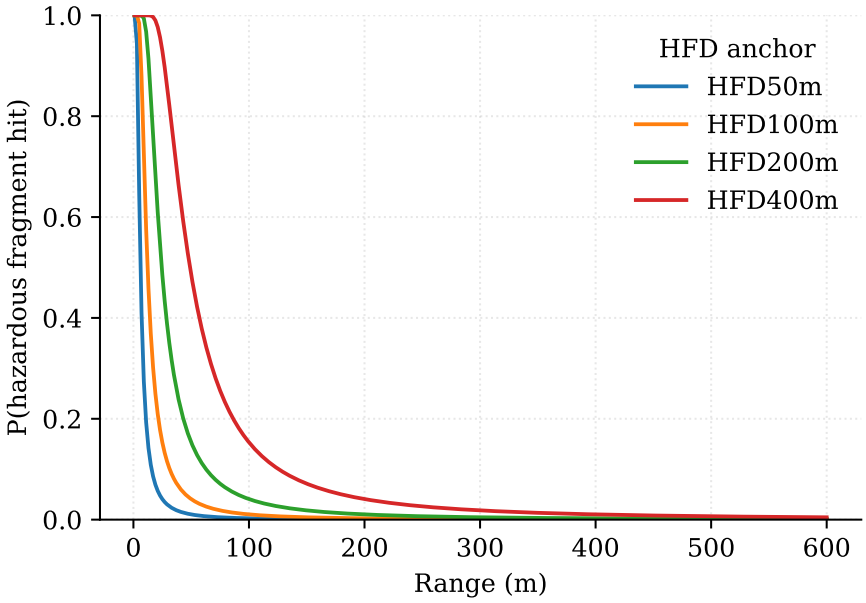

Figure 3. Probability of a hazardous-fragment strike versus range for four HFD anchors, from Equation 4 as implemented.

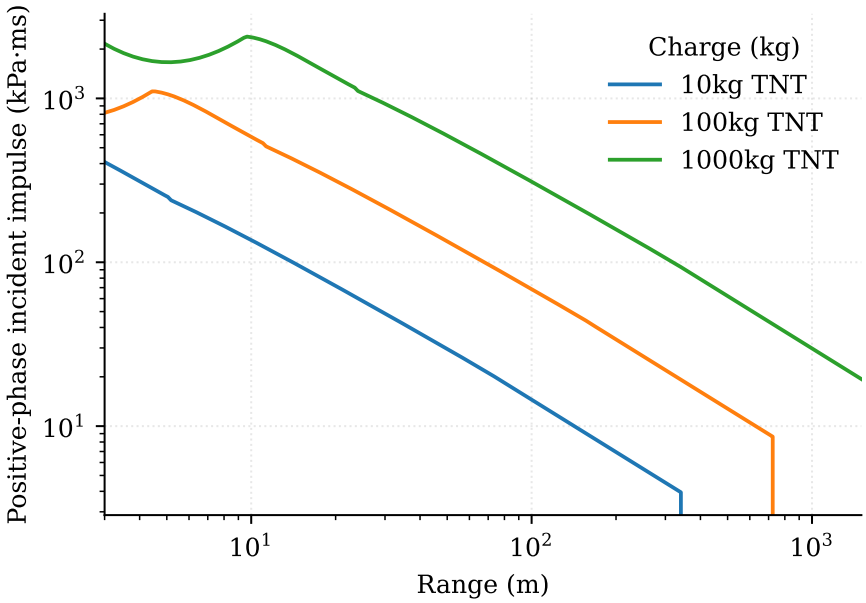

Figure 4. Positive-phase incident impulse versus range for three charge sizes, from the Kingery-Bulmash parametrisation as implemented.

3.6 Impulse-aware lethality

The lung-lethality estimate follows the Bowen iso-risk surface as expressed by the Joint Research Centre probit survey (Bowen et al., 1968; Karlos et al., 2019). Two intermediate quantities enter. The first is an effective pressure p_{eff} that accounts for reflection,

$$p_{\mathrm{eff}} = \frac{7\,p_s\,(p_s + 2p_0)}{2\,(p_s + 7p_0)}, \tag{5}$$

with p_0 the ambient pressure. The second is a scaled impulse

$$i_{\mathrm{sc}} = \frac{i}{\sqrt{p_0}\,m^{1/3}}, \tag{6}$$

with i the positive-phase impulse and $m = 70\,\mathrm{kg}$ the reference body mass. The lethality follows from a probit argument that combines the two,

$$y = 5.0 - 5.74\,\ln\!\left(\frac{4.2\,p_0}{p_{\mathrm{eff}}} + \frac{1.3}{i_{\mathrm{sc}}}\right), \qquad P_{\mathrm{lung}} = \Phi(y - 5), \tag{7}$$

so that lethality is high only when both the effective pressure is large and the scaled impulse is sufficient. The model also evaluates a pressure-only lethality as a log-normal probit anchored at the lethal thresholds of Table 1, and reports the higher of the two as the governing value together with a flag for which track governs. The contrast between the two tracks is the subject of Section 4.

3.7 Combined exposure level

For a single glanceable severity, the model reduces the quantities above to an ordinal exposure level with five values, from clear through cordon, caution, and danger, to lethal. The level is the worse of a blast contribution, driven by the overpressure band, and a fragment contribution, driven by the hit probability, so that fragment hazard escalates the level even where overpressure is mild. Inside the outer cordon or fragment ring but below any injury threshold, the level is set to cordon rather than clear, so that being inside a ring is never displayed as safe.

3.8 Position smoothing

Because $p_s(R)$ is steep near the charge, the model smooths the input position with an exponential moving average before computing any output. For a smoothing factor $\alpha \in (0, 1]$ and a raw fix sequence x_k, the smoothed position is

$$\hat{x}_k = \hat{x}_{k-1} + \alpha\,(x_k - \hat{x}_{k-1}), \tag{8}$$

initialised at the first fix. Smoothing the position rather than each output keeps distance, bearing, and overpressure mutually consistent, because all three are recomputed from one smoothed coordinate. The factor α trades responsiveness against stability, and we examine that trade in Section 4.

4 Results and Validation

4.1 Overpressure and eardrum response

Figure 1 confirms the steep near-field rise of overpressure and locates the injury bands on the range axis for a large charge. The structural band reaches out to a few hundred metres, while the lethal band is confined to the near field. Figure 2 shows that eardrum rupture probability rises through its transition over a band of ranges that depends on charge size, and that for a small charge the eardrum response saturates only very close in. The eardrum curve is useful precisely because it is graded across a region where the lung is not yet at risk.

4.2 Fragment risk rises faster than blast

Figure 3 shows the inverse-square growth of fragment-hit probability. For a given HFD, the probability is near the one-percent anchor at the HFD and climbs steeply inward, reaching tens of percent at half the HFD. The operational point is that a responder can be in a region of low overpressure, well short of the lung band, while already carrying a substantial fragment-hit probability. A model that reported only overpressure would understate the danger in exactly this region, which is why the combined exposure level takes the worse of the two contributions.

4.3 Pressure-only over-states lung lethality

Figure 5 contrasts the pressure-only and impulse-aware lethality tracks for a 100 and a 1000 kg charge over the near field. The figure is restricted to the regime where the Bowen lung iso-risk surface is meaningful, namely overpressures up to about 2 MPa, because closer in the overpressure is so far past the lethal threshold that lethality is unity by inspection and the probit is extrapolated. Within that regime the pressure-only track saturates to near certainty across a wide band, while the impulse-aware Bowen track is markedly lower and falls off sooner. For the 100 kg charge the Bowen track stays near zero throughout the model-valid regime, because the positive-phase pulse is too short to drive the lung to a lethal dose at these overpressures. The gap between the two tracks is the over-statement that a pressure-only readout would present to the responder.

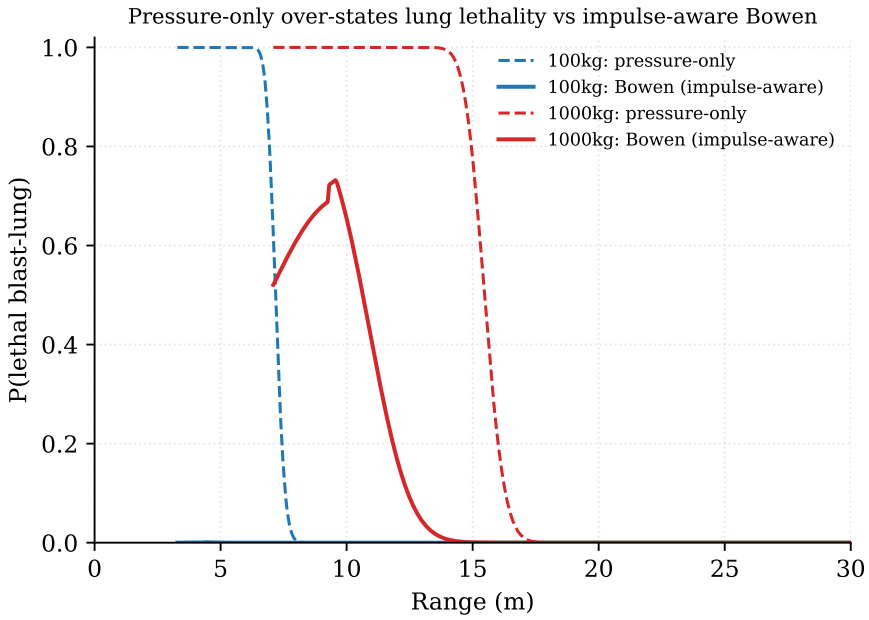

Figure 5. Blast-lung lethality versus range for 100 and 1000 kg charges. Pressure-only (dashed) saturates across a wide near-field band; the impulse-aware Bowen estimate (solid) is markedly lower, and for the 100 kg charge it stays near zero within the model-valid regime. The gap is the over-statement that a pressure-only readout would present to the responder.

Why this matters on approach

For the same peak overpressure, a smaller charge is less lung-lethal because its pulse is shorter. A responder closing on a small device who is shown a pressure-only lethality figure is shown a number that is too high. Reporting the impulse-aware estimate alongside it keeps the readout honest about which hazard, overpressure or fragmentation, is the real driver at close range.

4.4 The banded exposure level

Figure 6 shows the combined exposure level for a representative 500 kg incident as the responder closes from 400 m. The level steps up through cordon, caution, and danger, reaching lethal only in the near field, and the inner working line (K50) is marked for reference. The step structure is what the responder sees as a single colour-coded indicator, and it combines the continuous quantities above into one ordinal reading. Because the level takes the worse of the blast and fragment contributions, the transitions in the figure reflect whichever hazard governs at each range.

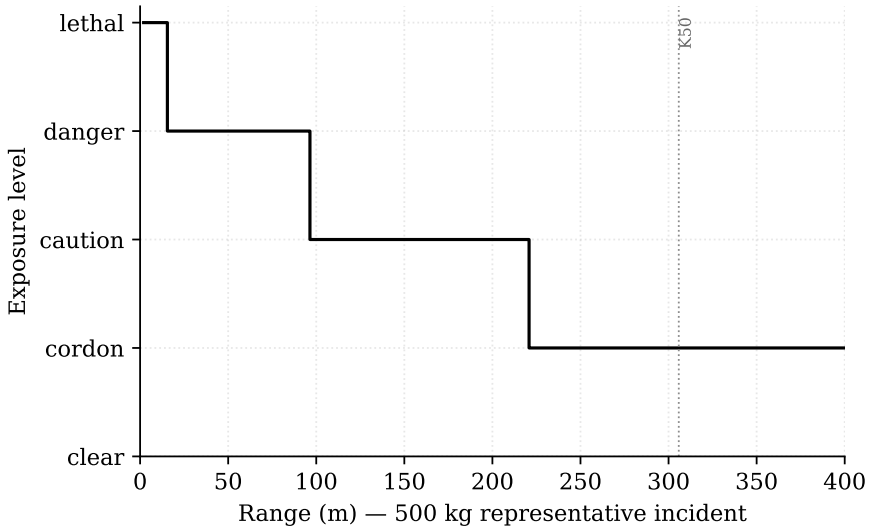

Figure 6. Combined exposure level versus range for a representative 500 kg incident, from the shipped exposure engine. The view is clamped to 400 m to show the severity transitions; the cordon level holds out to the much larger outer ring.

4.5 Position smoothing trade-off

Figure 7 characterises the smoother of Equation 8 with its step response, the settling of the displayed range after an instantaneous jump of the input from zero to 100 m. A small α rejects jitter strongly but lags the true range over many fixes, while a large α tracks quickly but admits more of the raw noise. Table 2 summarises the trade. The shipped default sits at $\alpha = 0.3$, where the lag is a few fixes, unnoticeable on foot, and the readout no longer flickers in the steep near-field region. The smoother acts on the position, not on the derived quantities, so the stability it provides is shared consistently by distance, bearing, and overpressure.

Table 2. Qualitative smoothing trade-off across the smoothing factor α.

α	Jitter rejection	Tracking lag
0.1	Strong	Many fixes
0.3	Balanced (shipped default)	A few fixes
0.6	Weak	Near-immediate

5 Implementation and Traceability

Every quantity in this paper is implemented once, in a shared library (`eod_core`), and consumed unchanged by both the phone companion and the wrist-worn approach display. The figures

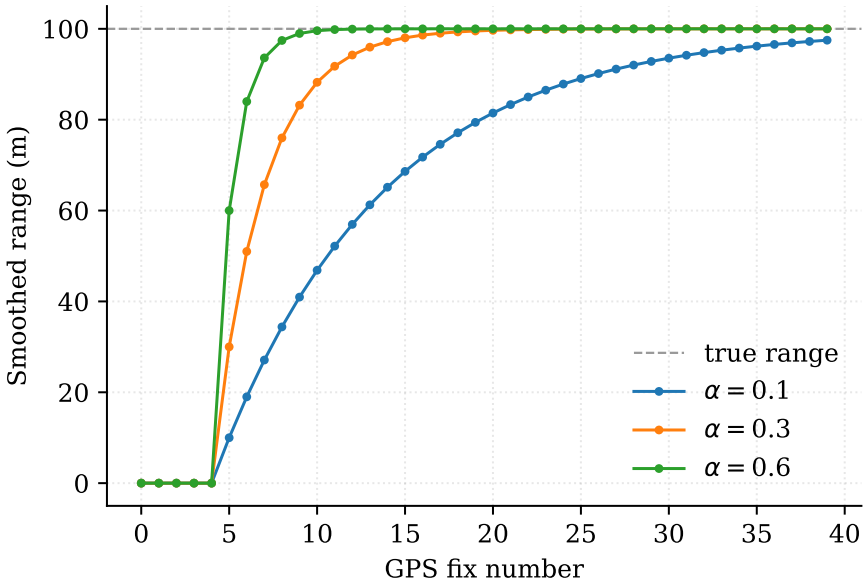

Figure 7. Exponential-moving-average step response for three smoothing factors, from the shipped smoother. The input jumps from 0 to 100 m at the fifth fix.

were not redrawn from the equations by hand. They were produced by an export routine that calls the same library functions the field application calls, writes the resulting series to a data file, and renders them. A curve in this paper and the value shown on the responder's display therefore originate in the same code path. The injury correlations, the fragment model, the impulse parametrisation, and the smoother are each a single function with an explicit validity band, and each suppresses its output rather than extrapolating when a fix falls outside that band.

6 Limitations and Threats to Validity

Several limitations bound the interpretation of the model. The injury probits are referenced to a 70 kg body mass and to idealised orientation assumptions, so individual outcomes will vary around the reported probabilities. The fragment model reports the probability of a hit, not the probability of injury given a hit, so it characterises exposure to the hazard rather than the wounding outcome. The air-blast and impulse correlations each have a validity band, and the model clamps or suppresses outputs outside it rather than extrapolating, which means the displayed values in the extreme near field are deliberately conservative placeholders rather than precise readings. Position accuracy is bound by the satellite fix, and the smoother trades a small lag for stability, so a fast approach will see the readout trail the true range by a few fixes. Finally, the combined exposure level is an ordinal reduction of continuous quantities and is intended as a glanceable indicator, not as a measurement. The model informs the responder. It does not authorise movement, and it does not replace command explosive-safety authority.

7 Future Work

Three extensions are natural. The first is a probability-of-injury-given-hit layer over the fragment model, which would convert the current hit probability into a wounding estimate using established penetration criteria. The second is a terrain-aware overpressure and fragment model that accounts for cover and line of sight, which would refine the near-field picture where a responder may be shielded. The third is per-responder calibration of the smoother, adapting α to the observed fix

noise and movement speed so that the lag is minimised for the conditions actually present.

8 Conclusion

A responder approaching a device is best served by a live, honest picture of their own exposure. By combining overpressure and its injury bands, fragment-hit probability, positive-phase impulse, and an impulse-aware lethality estimate from one shared engine, and by stabilising the readout for a wrist-worn device, the approach-exposure model provides that picture. Two findings stand out. Fragment risk rises as the inverse square of range and dominates the last tens of metres, and pressure-only lethality over-states the lung hazard for small charges because it ignores the short positive-phase pulse. Both are properties of established models, surfaced live from the same code that sizes the cordon. The final paper in the series addresses what happens when more than one incident is live at once and the responder's attention must be assigned.

References

Baker, W. E., Cox, P. A., Westine, P. S., Kulesz, J. J., & Strehlow, R. A. (1983). *Explosion hazards and evaluation*. Elsevier.

Bowen, I. G., Fletcher, E. R., & Richmond, D. R. (1968). *Estimate of man's tolerance to the direct effects of air blast* (tech. rep. No. DASA-2113). Defense Atomic Support Agency.

Brode, H. L. (1955). Numerical solutions of spherical blast waves. *Journal of Applied Physics*, *26*(6), 766–775. https://doi.org/10.1063/1.1722085

Department of Defense Explosives Safety Board. (2009). *Fragment and debris hazards* (tech. rep. No. Technical Paper No. 12). Department of Defense Explosives Safety Board.

Glasstone, S., & Dolan, P. J. (1977). *The effects of nuclear weapons* (3rd ed.). U.S. Department of Defense; U.S. Department of Energy.

Karlos, V., Solomos, G., & Larcher, M. (2019). *Analysis of the blast wave decay coefficient and survey of probit functions for blast injury* (tech. rep. No. JRC119310). European Commission, Joint Research Centre.

Kingery, C. N., & Bulmash, G. (1984). *Airblast parameters from TNT spherical air burst and hemispherical surface burst* (tech. rep. No. ARBRL-TR-02555). U.S. Army Ballistic Research Laboratory. Aberdeen Proving Ground, MD.

Mills, C. A. (1987). The design of concrete structures to resist explosions and weapon effects. *Proceedings of the 1st International Conference on Concrete for Hazard Protection*.

U.S. Department of Defense. (2019). *DoD ammunition and explosives safety standards* (tech. rep. No. DESR 6055.09). Defense Explosives Safety Regulation.

U.S. Department of Homeland Security & Bureau of Alcohol, Tobacco, Firearms and Explosives. (2016). *DHS/ATF bomb threat standoff card* (tech. rep.). U.S. Department of Homeland Security.